

NASA TECHNICAL  
MEMORANDUM



NASA TM X-1854

NASA TM X-1854

CAVITATION PERFORMANCE OF  
LINE-MOUNTED  $80.6^\circ$  HELICAL  
INDUCER IN HYDROGEN

*by Royce D. Moore and Phillip R. Meng*

*Lewis Research Center*

*Cleveland, Ohio*

CAVITATION PERFORMANCE OF LINE-MOUNTED 80.6°  
HELICAL INDUCER IN HYDROGEN

By Royce D. Moore and Phillip R. Meng

Lewis Research Center  
Cleveland, Ohio

NATIONAL AERONAUTICS AND SPACE ADMINISTRATION

---

For sale by the Clearinghouse for Federal Scientific and Technical Information  
Springfield, Virginia 22151 - CFSTI price \$3.00

## ABSTRACT

The noncavitating and cavitating performance of a line-mounted  $80.6^\circ$  helical inducer was determined in hydrogen over a liquid temperature range of  $34.1^\circ$  to  $42.2^\circ$  R ( $18.9$  to  $23.4$  K) and a flow coefficient range of  $0.08$  to  $0.12$  at rotative speeds of  $25\ 000$  and  $30\ 000$  rpm. The tank pressure requirement for this line-mounted inducer was compared with that for the same inducer closely coupled to the tank. The tank pressure requirement was determined to be greater for the line-mounted inducer. Inducer net positive suction head requirement increased with increasing flow coefficient and rotative speed and decreased with increasing temperature. Noncavitating head-rise coefficient, which decreased with increasing flow coefficient, was unaffected by temperature and rotative speed.



# CAVITATION PERFORMANCE OF LINE-MOUNTED 80.6°

## HELICAL INDUCER IN HYDROGEN

by Royce D. Moore and Phillip R. Meng

Lewis Research Center

### SUMMARY

The noncavitating and cavitating performance of an 80.6° helical inducer was determined in liquid hydrogen. The experimental inducer was installed in a line that extended 26.5 inches (67.3 cm) upstream of the blade leading edges. The net positive suction head NPSH requirements of the inducer were determined over a liquid temperature range of 34.1° to 42.2° R (18.9 to 23.4 K) and a flow coefficient range of 0.08 to 0.12 at rotative speeds of 25 000 and 30 000 rpm. The tank NPSH requirements for this line-mounted inducer were compared with those for the same inducer closely coupled to the tank. The tank NPSH requirements were determined to be greater for the line-mounted inducer because of the increased pressure losses in the longer inlet line. For a constant rotative speed, the required NPSH for the inducer operated at a given performance level decreased with increasing temperature and increased with increasing flow coefficient. For a given liquid temperature and flow coefficient, the magnitude of the required NPSH was greater at 30 000 rpm than at 25 000 rpm. When the condition of vapor at the inducer inlet was experienced, the inducer was capable of producing a satisfactory head rise for all liquid temperatures studied at 25 000 rpm; but at 30 000 rpm, the inducer produced a useful head rise for liquid temperatures above 40° R (22.2 K). The noncavitating head-rise coefficient, which decreased almost linearly with increasing flow coefficient, was unaffected by liquid temperature and rotative speed.

### INTRODUCTION

The inducer in a rocket engine turbopump is designed to operate satisfactorily with cavitation present on the suction surface of the blades. The evaporative cooling in the cavitation process causes the vapor pressure of the liquid surrounding a cavity to be reduced by an amount corresponding to the local temperature reduction. The pressure

within the cavity is reduced by a corresponding amount. This reduction in cavity pressure is equal to the change in the net positive suction head NPSH requirement for the inducer (refs. 1 to 4), where net positive suction head is defined as total pressure head above fluid vapor pressure head at the inducer inlet. Because of the evaporative cooling, the NPSH requirement of the inducer is less than it would be if the cooling did not occur. The amount of cooling realized is a function of the liquid, its temperature, the rotative speed and flow rate at which the inducer is operated, and also the geometric design of the inducer.

In hydrogen-fueled rocket vehicles, large volume tanks are required to contain the low-density liquid hydrogen. The weight of these fuel tanks and thus the payload capability is sensitive to the tank pressure. It is therefore desirable to design the tanks for the lowest pressure that will satisfy the inlet pressure requirements of the turbopump. The cavitating inducer is used ahead of the main pump to reduce the tank pressure requirements. The turbopump is usually installed in a line downstream from the fuel tank. Thus, line entrance pressure losses and pressure losses encountered in the line from the tank to the pump must be considered. These pressure losses will increase the tank pressure requirements.

The type of line configuration used to provide the flow from the fuel tank to the turbopump will have an effect on the tank pressure. In a previous investigation (ref. 5), the NPSH requirements of an 80.6° helical inducer were determined over a range of liquid temperatures and flows. The inducer was closely coupled to the fuel tank, and the pressure losses from the tank to the inducer were considered negligible. In the present investigation, the same inducer was installed at the end of a 26.5-inch (67.3-cm) long inlet line.

The objective of this investigation was to determine the NPSH requirements for the 80.6° helical inducer installed in the longer inlet line and to compare the tank pressure requirements for this type of configuration with those for the closely coupled configuration. The experimental inducer was tested over a liquid temperature range of 34.1° to 42.2° R (18.9 to 23.4 K). Flow coefficient was varied from 0.08 to 0.12 at rotative speeds of 25 000 and 30 000 rpm. These tests were conducted at Plum Brook Station of NASA-Lewis Research Center.

## SYMBOLS

$g$	acceleration due to gravity, 32.2 ft/sec <sup>2</sup> (9.8 m/sec <sup>2</sup> )
$\Delta H$	inducer head rise, ft (m) of liquid
NPSH	net positive suction head, ft (m) of liquid
$U_t$	blade tip speed, ft/sec (m/sec)



$V_a$  average axial velocity immediately upstream of the inducer inlet, ft/sec (m/sec)  
 $\phi$  flow coefficient,  $V_a/U_t$   
 $\psi$  head-rise coefficient,  $g \Delta H/U_t^2$

Subscripts:

NC noncavitating

T tank

## APPARATUS PROCEDURE

### Test Inducer

The test rotor used in this investigation was a three-bladed, flat-plate helical inducer with a tip helix angle of  $80.6^\circ$ . The inducer had a tip diameter of 4.980 inches (12.649 cm) and a hub- to tip-diameter ratio of 0.496. Both the tip diameter and the diameter ratio were maintained constant across the rotor. Significant geometric features, as well as a photograph of the inducer are shown in figure 1. The leading edge of the inducer blades were faired on the suction surface only (see fig. 1).

### Test Facility

This investigation was conducted in the liquid hydrogen pump facility shown schematically in figure 2. The inducer was installed in a line that extends 26.5 inches (67.3 cm) above the blade leading edges. The inducer was located near the bottom of the 2500-gallon ( $9.5\text{-m}^3$ ) vacuum-jacketed research tank. A booster rotor located downstream of the inducer was used to overcome system losses. The flow path is down the inlet line, through the inducer and booster rotor to a collector scroll, and into a discharge line to the storage dewar. For test runs above  $36.5^\circ\text{R}$  ( $20.3\text{ K}$ ), the liquid was recirculated to the research tank to extend the run time.

The facility is the same as that described in references 1, 4, and 5. Except for the replacement of the short inlet line with the relatively longer line, overall configuration of the facility is identical to that described in reference 5.

### Test Procedure

The research tank was filled with liquid hydrogen from the storage dewar. Prior to each test, the hydrogen was conditioned to the desired liquid temperature by either

vacuum for the colder runs or by recirculating the liquid for the warmer runs. The tank was then pressurized to 10 psi ( $6.9 \text{ N/cm}^2$ ) above the liquid vapor pressure. When the desired rotative speed was attained, the tank pressure (NPSH) was slowly reduced until the head rise deteriorated because of cavitation. The flow rate and bulk liquid temperature were maintained essentially constant during each test run. The noncavitating performance was obtained by varying the flow rate while maintaining a constant rotative speed and liquid temperature. The tank pressure for the noncavitating runs was maintained at 15 psi ( $10.4 \text{ N/cm}^2$ ) above the liquid vapor pressure.

The location of the instrumentation used in this investigation is shown schematically in figure 3. The measured parameters and the estimated system accuracy are also listed in figure 3.

The liquid vapor pressure was measured with vapor pressure bulbs that were charged with hydrogen from the tank. One vapor pressure bulb was located at the entrance to the inlet line. Another vapor pressure bulb was utilized to measure vapor pressure at the inducer inlet. Tank pressure, measured in the ullage space, was used as the reference pressure for the differential pressure transducers. The liquid level above the inducer, measured by a capacitance gage, was added to the reference pressure to correct the differential pressures to the inducer-inlet conditions. An averaged hydrogen temperature at the inducer inlet was obtained from two platinum resistor thermometers. A shielded total-pressure probe located at midstream approximately 1 inch (2.54 cm) downstream of the test rotor was used to measure the inducer pressure rise. Pump flow rate was obtained with a venturi flowmeter which was calibrated in water.

The line vapor bulb pressure was subtracted from the measured line total pressure and converted to feet of head using the inlet fluid density to obtain the inducer NPSH. The differential pressure, measured directly between tank pressure and the line-inlet vapor bulb pressure, was converted to feet of head to obtain tank NPSH. The line losses were subtracted from tank NPSH to verify inducer NPSH. These losses were calculated by multiplying the line fluid velocity head by the line loss coefficient, which was determined to be 0.75 from a calibration in air.

## RESULTS AND DISCUSSION

### Noncavitating Performance

The noncavitating performance of the  $80.6^\circ$  helical inducer is shown in figure 4 where head-rise coefficient  $\psi_{\text{NC}}$  is plotted as a function of flow coefficient  $\phi$ . Several nominal hydrogen temperatures are shown for test rotative speeds of 25 000 and 30 000 rpm. As expected, neither liquid temperature nor rotative speed has any measurable



effect on the head-rise coefficient. As in reference 5, the head-rise coefficient decreases almost linearly with increasing flow coefficient.

## Cavitation Performance

The cavitation performance for the 80.6° helical inducer is shown in figures 5 and 6 where head-rise coefficient  $\psi$  is plotted as a function of NPSH. Several flow coefficients are presented for each nominal hydrogen temperature. The cavitation performance at a rotative speed of 25 000 rpm is presented in figure 5 and the performance at a rotative speed of 30 000 rpm is presented in figure 6. The solid portion of the curves in each figure represents the performance with no vapor at the inducer inlet. The dashed portion of some of the curves represents the cavitation performance with vapor present at the inducer inlet. Vapor was assumed to be present at the inducer inlet when the NPSH was equal to or less than the inlet fluid velocity head.

Even when there was vapor present at the inducer inlet, the inducer was capable of producing a satisfactory head rise at all temperatures for a rotative speed of 25 000 rpm (fig. 5). However, at a rotative speed of 30 000 rpm, the inducer could produce a satisfactory head rise only at liquid temperatures of 40.1° R (22.3 K) and above with vapor in the inducer inlet (fig. 6(e) to (g)). The head rise deteriorated almost immediately when vapor occurred at the inducer inlet at liquid temperatures of 36.6° to 39.1° R (20.3 to 21.7 K) (see fig. 6(b) to (d)).

Several general trends can be observed from the curves of figures 5 and 6. First, for a given hydrogen temperature and rotative speed, the required NPSH for a given performance level decreased with decreasing flow coefficient. For a given flow coefficient and rotative speed, the required NPSH decreased with increasing liquid temperature. These two trends were also observed in reference 5. For a given flow coefficient and liquid temperature, the required NPSH increased substantially as the rotative speed was increased from 25 000 rpm to 30 000 rpm.

These trends are summarized in figures 7 and 8 where the required net positive suction head for a head-rise coefficient ratio ( $\psi/\psi_{NC}$ ) of 0.70 is plotted as a function of flow coefficient  $\phi$ . The required NPSH is plotted for several nominal hydrogen temperatures at rotative speeds of 25 000 rpm (fig. 7) and 30 000 rpm (fig. 8). When the NPSH is lowered to the inlet fluid velocity head, the inlet static pressure is equal to the inlet fluid vapor pressure. A further reduction in NPSH will cause the inlet fluid to boil and the liquid-vapor mixture to be ingested by the inducer. The cavitation performance with vapor present at the inducer inlet is represented by the dashed portion of the curves in figures 7 and 8. The solid portion of the curves in these figures represented the condition with no vapor present at the inducer inlet.



When there is no vapor at the inducer inlet, the required NPSH increased rapidly with increasing flow coefficient, and the required NPSH decreased significantly with increasing liquid temperature. These two trends are evident at both rotative speeds. The magnitude of the required NPSH is much greater at the higher rotative speed.

When there is vapor at the inducer inlet, the required NPSH increased (but not as rapidly as when there is no vapor at the inlet) with increasing flow coefficient. For a rotative speed of 25 000 rpm (fig. 7), the required NPSH continued to decrease to values below the inlet fluid velocity head with increasing liquid temperature. At 30 000 rpm with vapor at the inducer inlet (fig. 8), the required NPSH remained essentially equal to the inlet fluid velocity head for liquid temperatures of  $36.6^{\circ}$  to  $39.1^{\circ}$  R ( $20.3$  to  $21.7$  K). As the temperature was increased to  $40.1^{\circ}$  R ( $22.3$  K), the required NPSH decreased to a value below the inlet fluid velocity head.

## Tank NPSH Requirements

A comparison of the tank pressure requirements for the closely coupled inducer (ref. 5) and those for the inducer mounted in the longer line is shown in figure 9. The required tank NPSH for an inducer head-rise coefficient ratio of 0.7 is plotted as a function of flow coefficient. The data shown for both configurations is for a liquid temperature of  $36.6^{\circ}$  R ( $20.3$  K) and a rotative speed of 30 000 rpm. For the entire flow range studied, the tank NPSH requirements are greater for the longer inlet line configuration than those with the closely coupled configuration. The greater tank required NPSH for the longer inlet line configuration was observed at all liquid temperatures studied. This is due to the greater losses associated with the longer inlet line.

The difference between the tank required NPSH curve of figure 9 for the longer inlet line configuration and the corresponding inducer required NPSH curve from figure 8 is a measure of the losses.

## SUMMARY OF RESULTS

The noncavitating and cavitating performance of an  $80.6^{\circ}$  helical inducer was evaluated in liquid hydrogen. The net positive suction head NPSH requirements were determined over a liquid temperature range of  $34.1^{\circ}$  to  $42.2^{\circ}$  R ( $18.9$  to  $23.4$  K) and a flow coefficient range of 0.08 to 0.12 at rotative speeds of 25 000 and 30 000 rpm. The experimental inducer was installed in a line which extended 26.5 inches (67.3 cm) above the blade leading edges. The tank pressure requirement for this inlet line configuration was compared with that for a closely coupled inducer. This investigation yielded the following principal results:

1. The tank NPSH requirement is greater for the inducer in the longer inlet line configuration as compared with that for the same inducer in the closely coupled configuration. This was attributed to the greater losses associated with the longer inlet line.

2. The inducer required NPSH for a given performance level decreased with increasing liquid temperature and increased with increasing flow coefficient. The required NPSH was greater for a rotative speed of 30 000 rpm as compared with that for 25 000 rpm.

3. When the condition of vapor at the inducer inlet was experienced, the inducer was capable of producing a satisfactory head rise for all liquid temperatures studied at 25 000 rpm. But at 30 000 rpm, the inducer produced a useful head rise only for liquid temperatures above  $40^{\circ}\text{R}$  ( $22.2\text{ K}$ ).

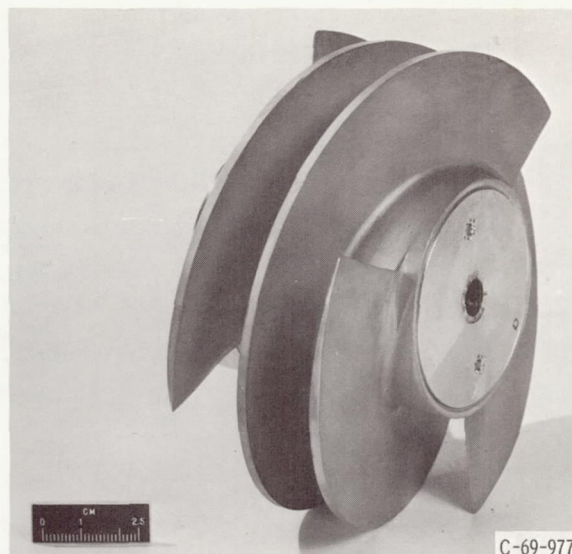
4. No measurable effect on the noncavitating head-rise coefficient was observed with liquid temperature or rotative speed. The noncavitating head-rise coefficient decreased almost linearly with increasing flow coefficient.

Lewis Research Center,  
National Aeronautics and Space Administration,  
Cleveland, Ohio, June 9, 1969,  
128-31-32-06-22.

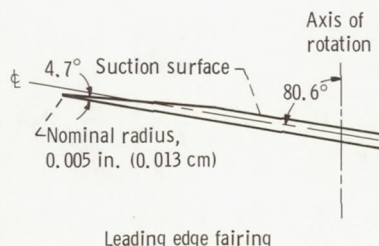
## REFERENCES

1. Meng, Phillip R.: Change in Inducer Net Positive Suction Head Requirement with Flow Coefficient in Low Temperature Hydrogen ( $27.9^{\circ}$  to  $36.6^{\circ}\text{R}$ ). NASA TN D-4423, 1968.
2. Ruggeri, Robert S.; Moore, Royce D.; and Gelder, Thomas F.: Method for Predicting Pump Cavitation Performance. ICRPG Ninth Liquid Propulsion Symposium. Vol. II. Rep. CPIA-155, vol. 2, Applied Physics Lab., Johns Hopkins Univ., Sept. 1967, pp. 129-144. (Available from DDC as AD-383825.)
3. Ruggeri, Robert S.; and Moore, Royce D.: Method for Prediction of Pump Cavitation Performance for Various Liquids, Liquid Temperatures, and Rotative Speeds. NASA TN D-5292, 1969.
4. Ball, Calvin L.; Meng, Phillip R.; and Reid, Lonnie: Cavitation Performance of  $84^{\circ}$  Helical Pump Inducer Operated in  $37^{\circ}$  and  $42^{\circ}\text{R}$  Liquid Hydrogen. NASA TM X-1360, 1967.
5. Meng, Phillip R.; and Moore, Royce D.: Cavitation Performance of  $80.6^{\circ}$  Helical Inducer in Liquid Hydrogen. NASA TM X-1808, 1969.





Tip helix angle (from axial direction), deg	80.6
Rotor tip diameter, in. (cm)	4.980 (12.649)
Rotor hub diameter, in. (cm)	2.478 (6.294)
Hub tip ratio	0.496
Number of blades	3
Axial length, in. (cm)	2.00 (5.08)
Peripheral extent of blades, deg	280
Tip chord length, in. (cm)	12.35 (31.37)
Hub chord length, in. (cm)	6.36 (16.15)
Solidity at tip	2.350
Tip blade thickness, in. (cm)	0.100 (0.254)
Hub blade thickness, in. (cm)	0.150 (0.381)
Calculated radial tip clearance at hydrogen temperature, in. (cm)	0.025 (0.064)
Ratio of tip clearance to blade height	0.020
Material	6061-T6 Aluminum



Leading edge fairing

Figure 1. - Photograph and geometric details of 80.6° helical inducer.

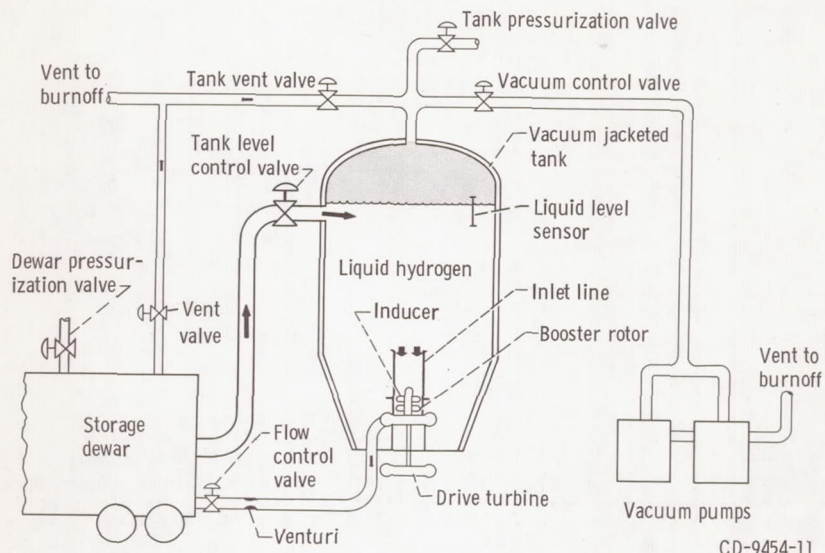
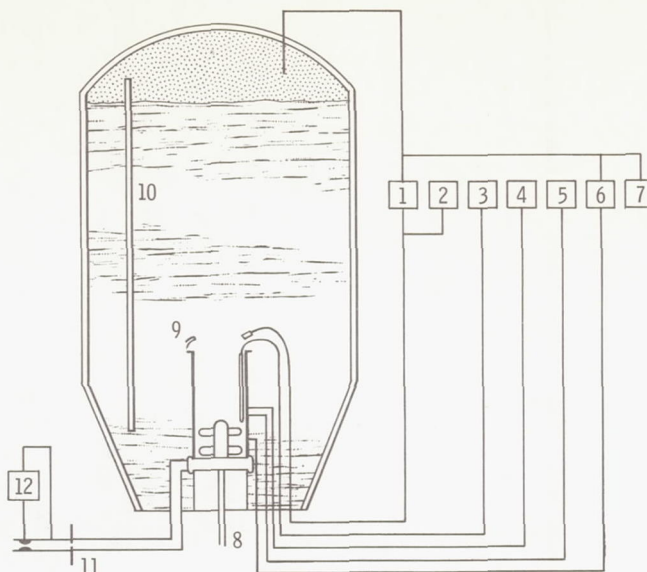


Figure 2, - Liquid hydrogen pump test facility.





Item number	Parameter	Estimated system accuracy	Number used	Remarks
1	Tank net positive suction head	Low } $\pm 0.05$ psi range } ( $0.035 \text{ N/cm}^2$ ) High } $\pm 0.25$ psi range } ( $0.17 \text{ N/cm}^2$ )	1 1	Measured as differential pressure (converted to head of liquid) between vapor bulb at line inlet and tank pressure corrected to line inlet conditions
2	Vapor pressure at line inlet	$\pm 0.25$ psi ( $0.17 \text{ N/cm}^2$ )	1	Vapor bulb charged with liquid hydrogen from research tank
3	Vapor pressure at inducer inlet	$\pm 0.25$ psi ( $0.17 \text{ N/cm}^2$ )	1	Long, small diameter vapor bulb with streamlined trailing edge aligned with flow stream to minimize bulb cavitation
4	Static pressure (line)	$\pm 0.05$ psi ( $0.035 \text{ N/cm}^2$ )	1	Average of three pressure taps ( $120^\circ$ apart) located 10.5 in. (26.7 cm) above inducer inlet
5	Total pressure (line)	$\pm 0.05$ psi ( $0.035 \text{ N/cm}^2$ )	1	Shielded total pressure probe located 0.065 in. (0.165 cm) in from wall and 10.5 in. (26.7 cm) upstream at inducer
6	Inducer pressure rise	$\pm 1.0$ psi ( $0.69 \text{ N/cm}^2$ )	1	Shielded total pressure probe at midpassage 1 in. (2.54 cm) downstream of inducer
7	Tank pressure	$\pm 0.5$ psi ( $0.35 \text{ N/cm}^2$ )	1	Measured in tank ullage and corrected to inducer inlet conditions for reference pressure for differential transducers
8	Rotative speed	$\pm 150$ rpm	1	Magnetic pickup in conjunction with gear on turbine drive shaft
9	Line inlet temperature	$\pm 0.1^\circ \text{ R}$ ( $0.06 \text{ K}$ )	2	Platinum resistor probes $180^\circ$ apart at inlet
10	Liquid level	$\pm 0.5$ ft ( $0.15 \text{ m}$ )	1	Capacitance gage, used for hydrostatic head correction to inducer inlet conditions
11	Venturi inlet temperature	$\pm 0.1^\circ \text{ R}$ ( $0.06 \text{ K}$ )	1	Platinum resistor probe upstream of venturi
12	Venturi differential pressure	$\pm 0.25$ psi ( $0.17 \text{ N/cm}^2$ )	1	Venturi calibrated in air

Figure 3. - Instrumentation for liquid hydrogen pump test facility.

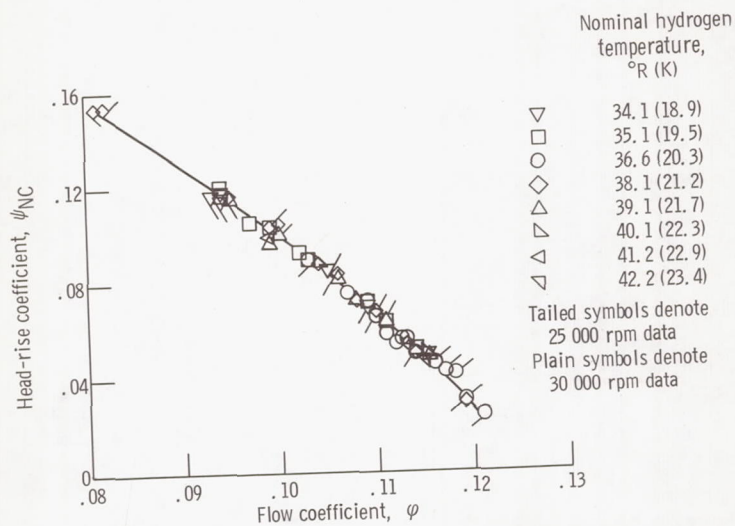


Figure 4. - Noncavitating performance of 80.6° helical inducer in hydrogen.



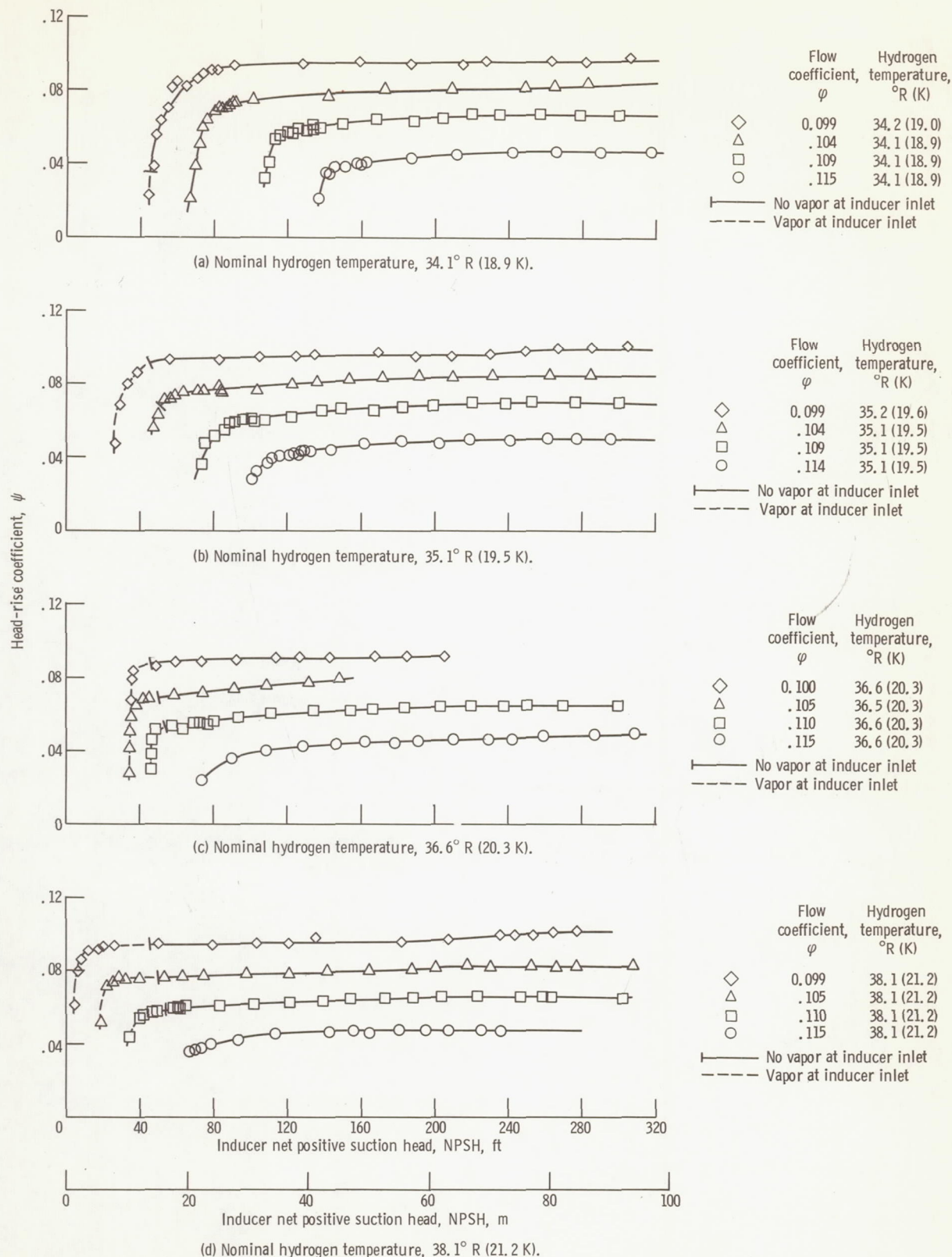


Figure 5. - Cavitation performance of 80.6° helical inducer in hydrogen at 25 000 rpm.

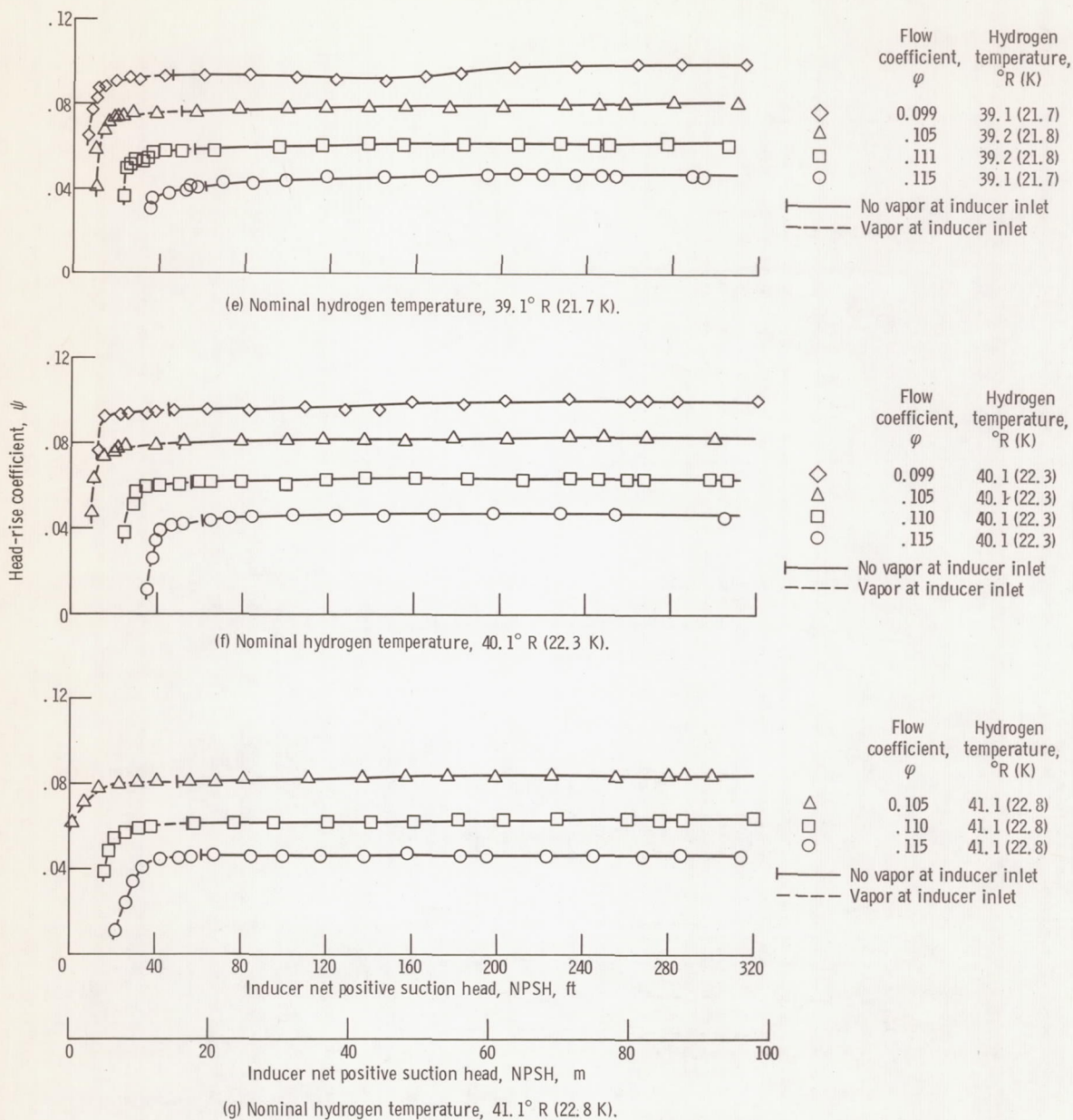


Figure 5. - Concluded.



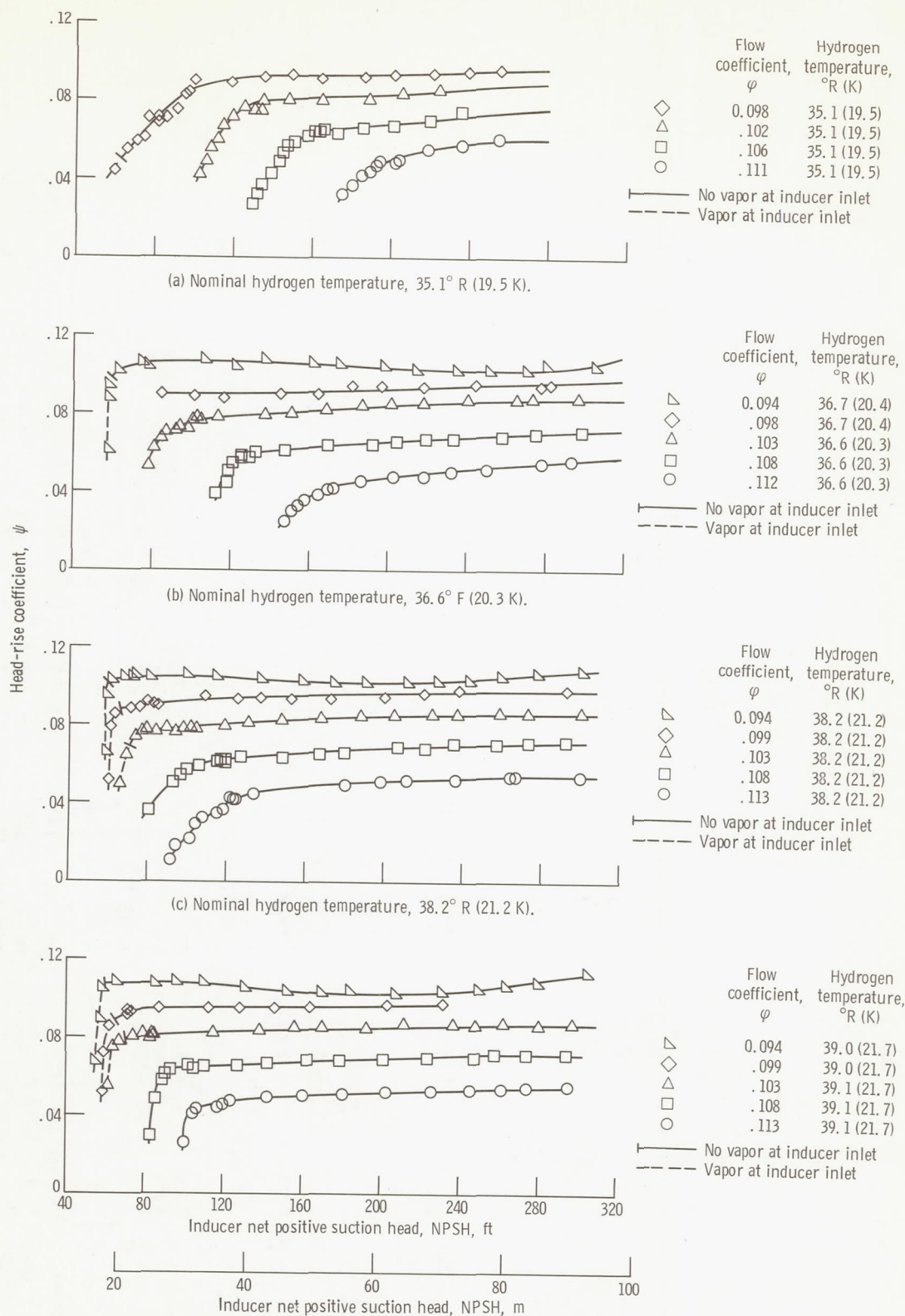


Figure 6. - Cavitation performance of 80.6° helical inducer in hydrogen at 30 000 rpm.

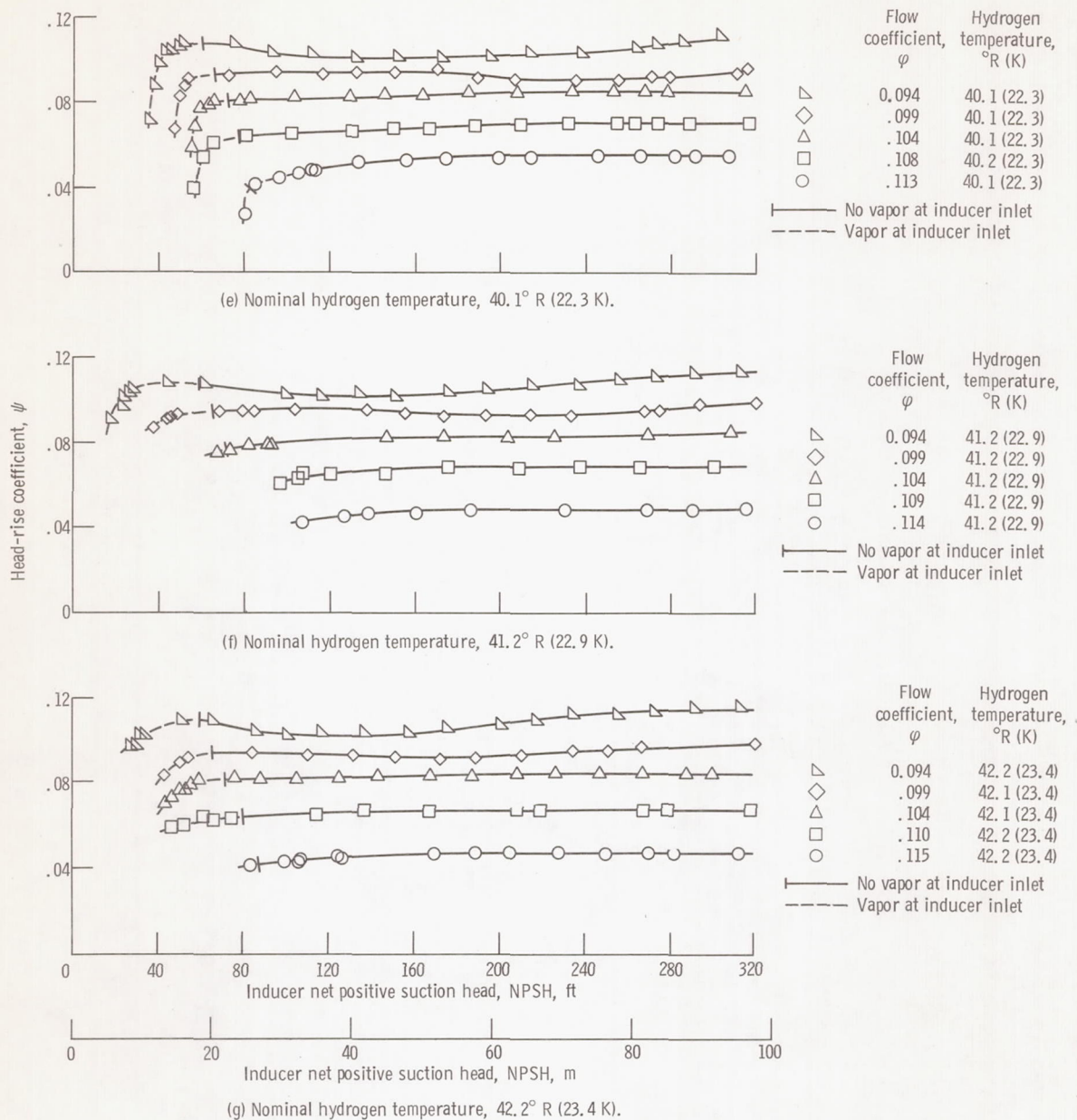


Figure 6. - Concluded.



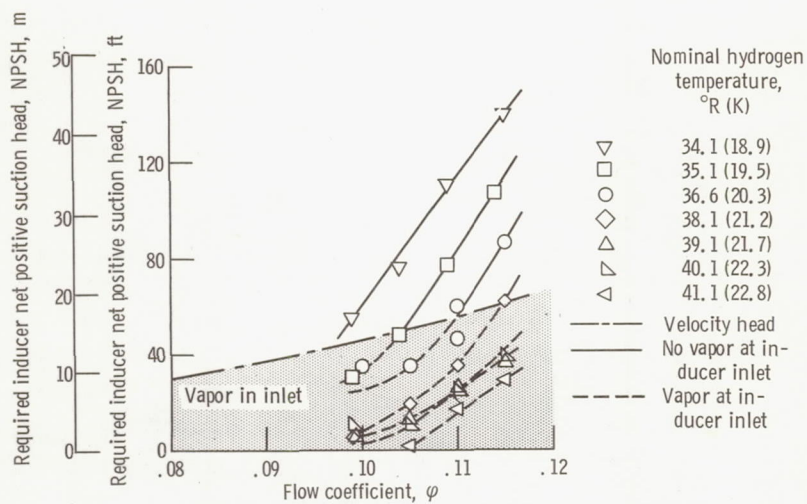


Figure 7. - Variation of inducer cavitation performance with flow coefficient at several hydrogen temperatures. Rotative speed, 25 000 rpm; head-rise coefficient ratio, 0.70.

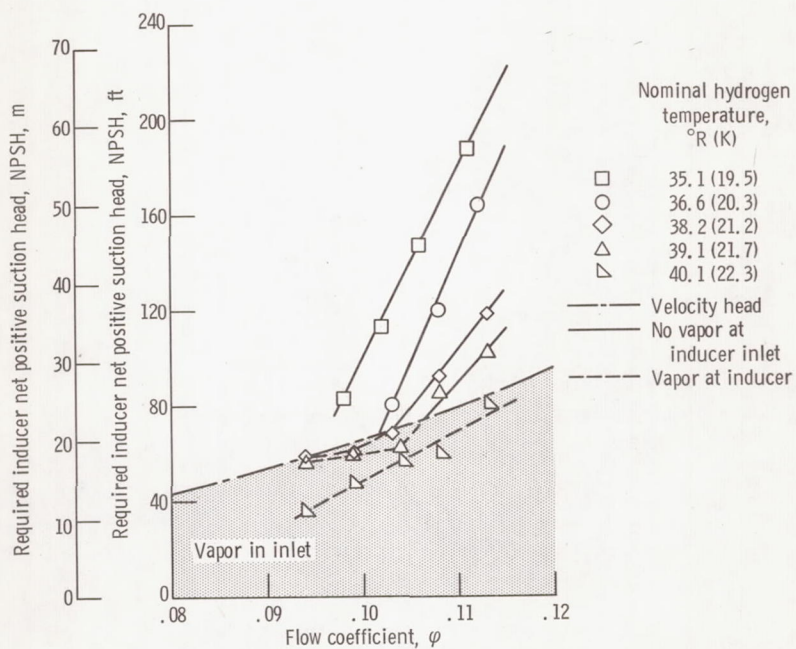


Figure 8. - Variation of inducer cavitation performance with flow coefficient at several hydrogen temperatures. Rotative speed, 30 000 rpm; head-rise coefficient ratio, 0.70.



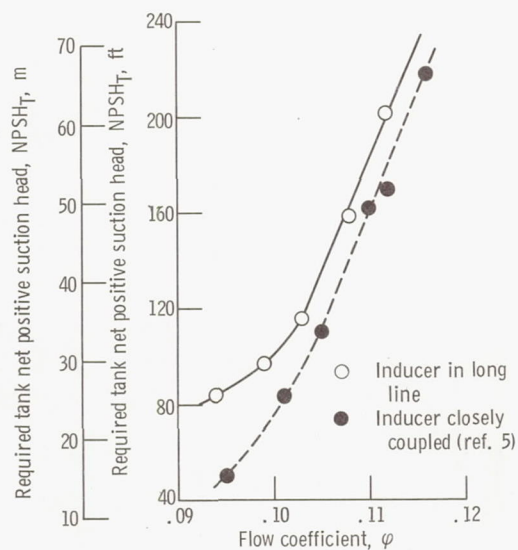


Figure 9. - Comparison of required tank net positive suction head for 80.6° helical inducer in two different inlet line configurations. Rotative speed, 30 000 rpm; liquid temperature, 36.6° R (20.3 K); inducer head-rise coefficient ratio, 0.70.